J Nanopart Res (2015) 17:330
DOI 10.1007/s11051-015-3136-9

RESEARCH PAPER

Control of size and aspect ratio in hydroquinone-based synthesis of gold nanorods

Carlo Morasso · Silvia Picciolini · Domitilla Schiumarini · Dora Mehn · Isaac Ojea-Jiménez · Giuliano Zanchetta · Renzo Vanna · Marzia Bedoni · Davide Prosperi · Furio Gramatica

Received: 22 May 2015 / Accepted: 25 July 2015 / Published online: 5 August 2015

Abstract In this article, we describe how it is possible to tune the size and the aspect ratio of gold nanorods obtained using a highly efficient protocol based on the use of hydroquinone as a reducing agent by varying the amounts of CTAB and silver ions present in the "seed-growth" solution. Our approach not only allows us to prepare nanorods with a four times increased Au^{3+} reduction yield, when compared with the commonly used protocol based on ascorbic acid, but also allows a remarkable reduction of 50–60 % of the amount of CTAB needed. In fact, according to our findings, the concentration of CTAB present in the seed-growth solution do not linearly influence the final aspect ratio of the obtained nanorods, and an optimal concentration range between 30 and 50 mM has been identified as the one that is able to generate particles with more elongated shapes. On the optimized protocol, the effect of the concentration of Ag^{+} ions in the seed-growth solution and the stability of the obtained particles has also been investigated.

Keywords Au nanorods · Plasmonics · CTAB · Hydroquinone · Nanoparticles

Introduction

Colloidal gold nanoparticles (AuNP) have attracted the attention of many scientists in the last 20 years due to their unique size- and shape-dependent optical and electronic properties combined with biological compatibility (Cobley et al. 2011). In addition, AuNP can be easily conjugated with biomolecules such as peptides, proteins, or nucleic acids that confer them in selectivity of action (Katz and Willner 2004). This fact strongly amplifies their potential and makes them

Electronic supplementary material The online version of this article (doi:10.1007/s11051-015-3136-9) contains supplementary material, which is available to authorized users.

C. Morasso (✉) · S. Picciolini · D. Schiumarini · R. Vanna · M. Bedoni · F. Gramatica
Laboratory of Nanomedicine and Clinical Biophotonics (LABION), Fondazione Don Carlo Gnocchi ONLUS, Via Capecelatro 66, 20148 Milan, Italy
e-mail: cmorasso@dongnocchi.it

D. Mehn · I. Ojea-Jiménez
Institute for Health and Consumer Protection (IHCP), European Commission Joint Research Centre, 21027 Ispra, VA, Italy

G. Zanchetta
Dipartimento di Biotecnologie Mediche e Medicina Traslazionale, Universitá degli Studi di Milano, via F.lli Cervi 93, 20090 Segrate, Italy

D. Prosperi
NanoBioLab, Dipartimento di Biotecnologie e Bioscienze, Università degli Studi di Milano Bicocca, Piazza della Scienza 2, 20126 Milan, Italy

a useful tool for a number of biomedical applications such as drug delivery (Han et al. 2007), light-triggered apoptosis (Pérez-Hernández et al. 2015), optoacustic imaging (Bao et al. 2013), and thermal and optical sensing of biomarkers (Howes et al. 2014; Polo et al. 2013).

Among the different nanostructures reported in the literature, anisotropic nanoparticles and particularly gold nanorods (AuNR) present several advantages in comparison with more conventional spherical nanoparticles. AuNR have two plasmon modes associated with the oscillation of electrons along the longitudinal and the transverse axes, respectively. Albeit the position of the band related to the transverse axis is basically in the same region of the most commonly prepared spherical nanoparticles (510–580 nm), the longitudinal band, which is more intense, can be tuned between 620 and 1200 nm, depending on the aspect ratio of AuNR (Chen et al. 2013). As this region matches the so called "biological window," where the absorption background in human tissues is negligible, this makes AuNR particularly suitable for in vivo applications among the realm of colloidal nanoparticles (Choi et al. 2011). In addition, AuNR are able to enhance optical signals, including Raman and luminescent signals, more efficiently than standard spherical nanoparticles (Saute et al. 2012; Partanen et al. 2015).

The most common protocol used for the preparation of AuNR is based on a two-step seed-mediated approach developed by Sau and Murphy (2004) involving a large amount of hexadecyl trimethylammonium bromide (CTAB) surfactant. In this method, a Au^{3+}–CTAB complex is formed and reduced by means of ascorbic acid in the presence of Ag^{+} ions combined with preformed Au^{0} seeds. Despite the many studies conducted so far, several shortcomings remain unsolved. The most deleterious drawback is the difficulty to fully remove the surfactant during surface modification with other molecules of interest, including biomolecules, PEGs, linkers, etc. (Soliman et al. 2015; Kinnear et al. 2014). This is particularly detrimental when AuNR are intended for use in biomedicine, because CTAB proved to be highly cytotoxic (Alkilany et al. 2009). A further important issue concerns the shape and size of the obtained nanoparticles, which strongly depend on the presence of traces of iodide impurities in CTAB, which is used in a large quantity. Therefore, different results are obtained using CTAB from different suppliers and even with different batches from the same supplier (Rayavarapu et al. 2010). Eventually, CTAB is expensive, as it accounts for more than half of the total cost of reagents and the yield of gold reduction is relatively low (about 20 %) (Ratto et al. 2010).

For all these reasons, the development of synthetic protocols which are more efficient, precise, and less dependent on the use of CTAB (or, ideally, that do not use this reagent at all) and the preparation of anisotropic plasmonic nanoparticles which are able to absorb light in the near infra-red (e.g. nanoprisms or nanostars) remain of great interest and are the subject of intensive research (Morasso et al. 2014; Pelaz et al. 2012; Scarabelli et al. 2013).

Materials and methods

Chemicals

All chemicals were purchased from Sigma-Aldrich (St. Louis, MO) and used as received. Water was deionized and ultra filtered using a MilliQ apparatus from Millipore Corporation (Billerica, MA) just before use.

Synthesis of gold nanorods

Seeds solution

5 mL solution of 0.2 M CTAB was prepared using the ultrasonication at 40 °C, in order to allow a complete dissolution of the surfactant and was mixed with 5 mL of 0.5 mM $HAuCl_4$. The temperature of the reaction was then kept constant at 27 °C, and 600 μL of $NaBH_4$ (10 mM) dissolved in water at 4 °C was added to the mixture under vigorous stirring. The solution rapidly changed color from yellow to brownish because of the formation of small gold nanoparticles. The solution was stirred for further 20 min before use.

Growth solution

Different amounts of CTAB (see Table 1) were dissolved together with 22 mg of hydroquinone (HQ) in 5 mL of water at 40 °C, using the ultrasonication to allow a complete dissolution of the surfactant. The mixture was then kept at 27 °C. Subsequently, 200 μL of a 4 mM $AgNO_3$ solution

Table 1 Amount of CTAB used for the production of different batches of AuNR

Concentration (mM)	Amounts (mg)	Concentration (mM)	Amounts (mg)
10	36.44	60	218.64
20	72.88	70	255.08
25	91.10	80	291.52
30	109.32	90	327.96
40	145.76	100	364.40
50	182.80		

and 5 mL of $HAuCl_4$ (1 mM) were added under vigorous stirring. Immediately after that, 12 μL of seed solution was added to the growth solution. The final mixture changed color and the reaction were stirred up to 3 h to complete the reaction depending on the concentration of CTAB present. AuNR were then centrifuged at 10,000 rpm for 10 min, resuspended in water, and characterized by UV–Vis spectroscopy and TEM.

Results and discussion

Hydroquinone base synthesis of AuNR

HQ is an aromatic molecule characterized by a weak reducing power, which has been proposed as an effective alternative to citrate and ascorbic acid for the preparation of AuNP of different sizes and shapes, especially in seed-mediated approaches (Perrault and Chan 2009; Mehn et al. 2013). Recently, Vigderman and Zubarev (2013) demonstrated that HQ can be successfully used for the preparation of AuNR characterized by high aspect ratio (a.r 6–8) with quantitative yield, suggesting that this synthetic route could become more effective than the one based on the use of ascorbic acid as a reducing agent.

In this work, we used HQ for the preparation of short AuNR (a.r. 2–4) and demonstrated the possibility to tailor the aspect ratio and the dimension of the obtained nanoparticles by varying the amounts of CTAB and Ag^+ added to the seed-growth solution. Our optimized protocol was based on a two-step approach. First, similarly to what is done in the standard method, small spherical Au seeds of 2–3 nm were prepared by an initial reductive step using $NaBH_4$ (Fig. S1 in Supporting information).

In the second step, a "seed-growth" solution was prepared mixing different amounts of CTAB (depending on the desired final size) with a fixed amount of HQ dissolving the powders by ultrasound assistance. Subsequently, a solution containing Au^{3+} and Ag^+, necessary to induce the symmetry break of nascent nanoparticles once they reached a size of 5–6 nm (Walsh et al. 2015), was added under vigorous stirring. Finally, a small amount of seeds were added to the solution and, after a few minutes, the solution began to gain color because of the formation of AuNR. The reaction was then left under stirring until the position of the spectrophotometric longitudinal plasmon peak reached a maximal intensity. UV–Vis spectra exhibit the characteristic double peak of rod-shaped nanoparticles corresponding to the two different dimensions of the AuNR and, similarly to what previously reported for long AuNR (Vigderman and Zubarev 2013), the amount of particles obtained, monitored by UV–Vis spectroscopy, was find to be about four times higher than the one achieved using ascorbic acid despite an identical concentration of Au^{3+} ions in the starting growth solution (Fig. 1).

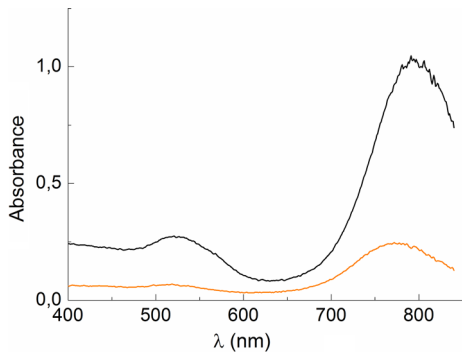

Fig. 1 UV–Vis spectra of Au NR obtained using the present method based on hydroquinone and 50 mM CTAB (*black*), and using the standard protocol based on ascorbic acid and 100 mM CTAB (*orange*). Both samples were diluted 5 times in water before the measurement. (Color figure online)

Influence of CTAB concentration on AuNR size and aspect ratio

In the first part of this study, we have investigated the possibility to decrease the amount of CTAB necessary to obtain AuNR taking advantage of the use of HQ as a reducing agent. In fact, it was previously reported that aromatic molecules derived from salicylic acid can influence the packing density of CTAB, and thus, they could be used to minimize the amount of surfactant needed for the preparation of AuNR (Ye et al. 2012).

HQ molecular structure is very simple and does not bear any carboxyl groups. As a consequence, HQ is not able to interact with the quaternary amine of CTAB, as proven by the fact that the viscosity of the suspension did not change in the presence of HQ (Fig S2 in Supporting information). However, the kinetics of the reaction, as well as the size and aspect ratio of the AuNR obtained were strongly dependent on the concentration of CTAB in the growth solution.

A shift of the longitudinal plasmonic peak towards higher λ values was observed in the CTAB lower range of concentrations (i.e., between 10 and 50 mM) corresponding to AuNR with higher aspect ratio (a/r) (Fig. 2a). In particular, TEM images in Fig. 3a–c show that AuNR obtained under these conditions were characterized by a similar width of about 13–15 nm and a length that varied from 27 nm ($a/r \approx 2$) using 10 mM CTAB (Fig. 3a) to 55 nm ($a/r \approx 3$) obtained in the range between 30 and 50 mM CTAB concentration, where a rather constant aspect ratio was obtained (Fig. 3g) (histograms with aspect ratio and length of each sample can be found in Fig. S3 in Supporting information).

Surprisingly, once the concentration of CTAB was further increased, the position of the longitudinal plasmonic peak shifted back to lower wavelengths (Fig. 2b). The analysis of TEM images for these sets of samples shows that, within this range of concentration, the length of the obtained rods still seems to gradually increase to 80 and 90 nm when 80 and 100 mM CTAB were used, respectively (Fig. 3e, f). However, the rod width also changed and AuNR became much larger and, as a consequence, the aspect ratio decreased. This set of data suggests that there is an optimal concentration of CTAB (about 50 mM) that promotes the formation of anisotropic nanostructures. Both below and above this "ideal" concentration, AuNR were characterized by a similar lower aspect ratio even if it is due to different sizes.

In particular, at low CTAB concentrations, the nanoparticles were much smaller than the ones obtained with a high amount of CTAB, where a progressive increment of the width was observed. These differences in nanoparticle size also reflect kinetic factors as shown in Fig. 4. AuNR with similar a/r values, such as those obtained using 25 and 70 mM CTAB, required different reaction times to be synthesized. Indeed, while the former reaction was completed in about 20 min, the latter needed at least 1 h before reaching a colloidal stabilization.

Influence of Ag^+ concentration on AuNR size and aspect ratio

We also studied the influence of the concentration of silver ions on the formation of AuNR by means of HQ (Fig. 5) as the use of a different amount of Ag^+ is the

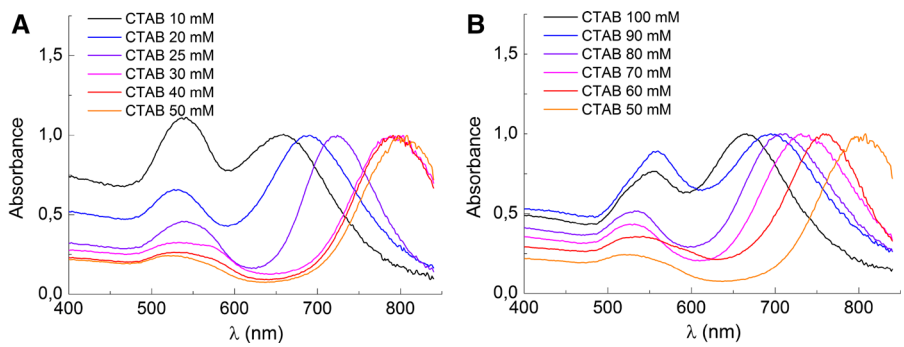

Fig. 2 UV–Vis spectra of AuNR obtained using different concentrations of CTAB: **a** CTAB concentrations in the range 10–50 mM. **b** CTAB concentrations in the range 50–100 mM. Spectra have been normalized in order to have the maximum of the longitudinal plasmonic band equal to 1

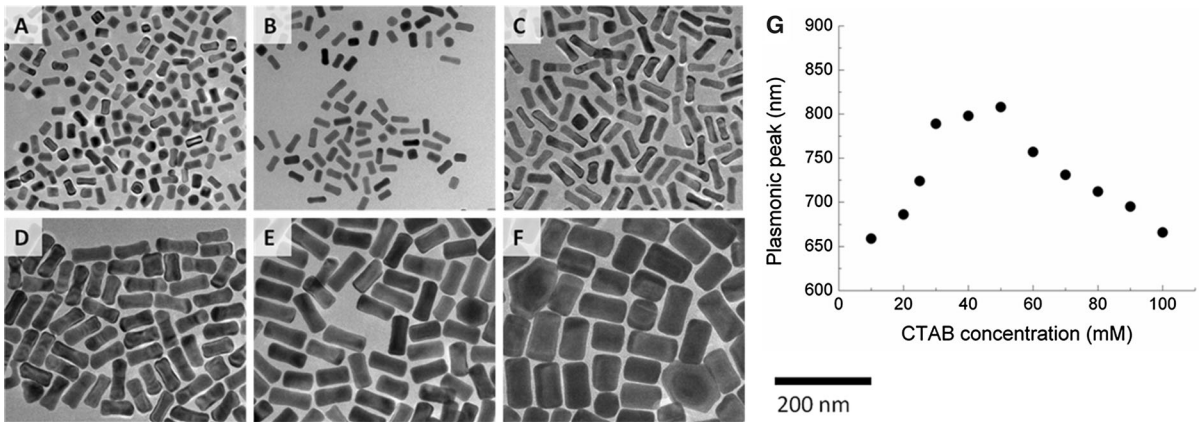

Fig. 3 TEM images of AuNR obtained using CTAB at **a** 10 mM; **b** 20 mM; **c** 40 mM; **d** 60 mM; **e** 80 mM; **f** 100 mM; **g** position of the longitudinal plasmonic peak as a function of the concentration of CTAB added to the seed-growth solution (TEM images of the complete series of AuNR can be found in Fig. S4 in Supporting information)

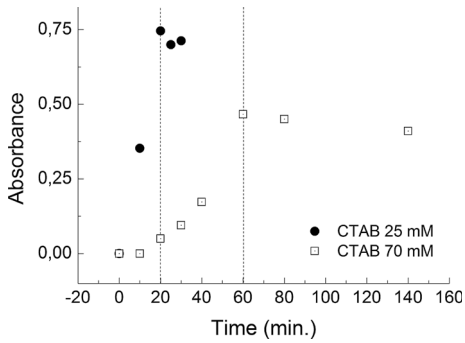

Fig. 4 Variation of the intensity of the longitudinal plasmonic peak during the synthesis of AuNR using different amounts of CTAB in solution

most common approach used to tailor the *a*/*r* of nanoparticles in the standard approach based on ascorbic acid. When a small amount of 4 mM $AgNO_3$ solution (100 μL) was used, the AuNR exhibited a longitudinal band at 660 nm that corresponds to an *a*/*r* of about 2 (Fig. 5c). Using a higher amount of silver ions, it was possible to produce longer AuNR and the plasmonic band was shifted to 740 nm ($a/r \approx 3$) and 800 nm ($a/r \approx 3.3$) when 150 and 200 μL of 4 mM $AgNO_3$ solution, respectively, were added to the seed-growth solution. TEM images in Fig. 5a–c suggested that the main driving factor behind the difference in the aspect ratios was a variation in the width of the AuNR (from 16 to 25 nm). (Histograms with aspect ratio and length of each sample can be found in Fig. S5 in Supporting information.) This trend was very similar to the one observed in the synthesis with ascorbic acid and suggested a similar role of Ag^+ ions in both protocols.

Stability of AuNR

At last, we studied the stability of the obtained particles. Once that the AuNR have been centrifuged and resuspended in water, they can be stored at room temperature without any major sign of aggregation for several months and they appear just to slightly decrease their aspect ratio probably because of the Ostwald ripening (Fig. 6a) (Zou et al. 2010). Besides, we also tested the stability of the AuNR here obtained in more harsh conditions such as phosphate buffer saline (PBS), a buffer used in biological research, and fetal bovine serum (FBS), a common supplement used in many cell cultures. Similarly to what previously observed with the standard AuNR obtained by means of ascorbic acid (Huang et al. 2009), the UV–Vis spectra analysis (Fig. 6b, c) shows that the here prepared AuNR are stable for 48 h in FBS, while a progressive aggregation is observed in PBS.

On the contrary, if AuNR are centrifuged and resuspended in water more than three times, they quickly began to aggregate and the suspension becomes dark as the surface coating of CTAB is destabilized and is not able to keep the particles dispersed anymore.

Conclusions

To summarize, in the present article, we have developed and optimized a protocol for a high-yield preparation of AuNR based on the use of HQ as a

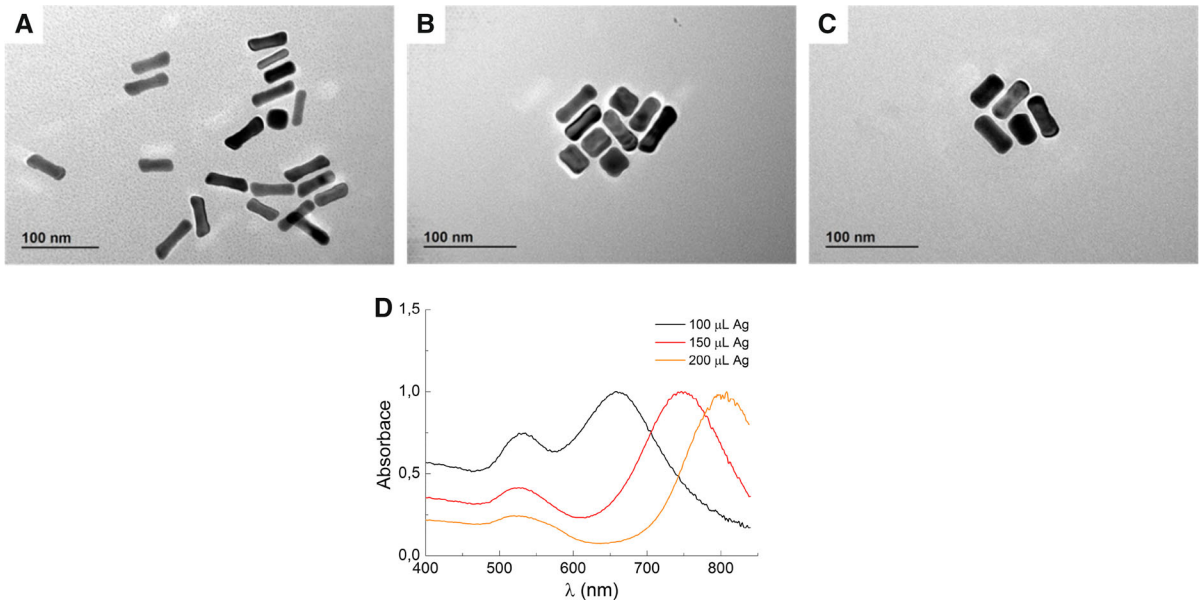

Fig. 5 *Top* TEM images of AuNR obtained using 50 mM CTAB and different amounts of 4 mM Ag^+ ions in the seed-growth solution. **a** 200 μL; **b** 150 μL; **c** 100 μL; **d** UV–Vis spectra of the AuNR. Spectra have been normalized in order to have the maximum of the longitudinal plasmonic band equal to one

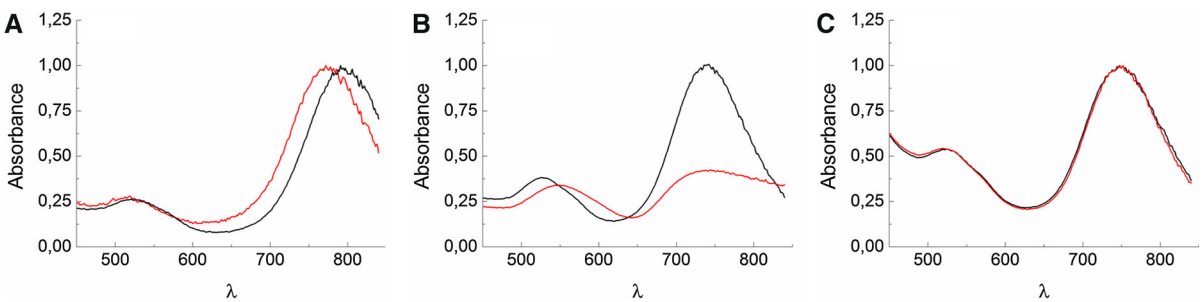

Fig. 6 **a** UV–Vis spectra of AuNR immediately after being obtained (*black*) and after 6 months stored at room temperature (*red*). **b** UV–Vis spectra of AuNR in PBS immediately after being redispersed (*black*) and after 48 h (*red*). **c** UV–Vis spectra of AuNR in FBS immediately after being redispersed (*black*) and after 48 h (*red*). Spectra have been normalized in order to have the maximum of the longitudinal plasmonic band equal to one. (Color figure online)

reducing agent. The effect of the concentration of CTAB and Ag^+ ions in the seed-growth solution was studied and we demonstrated how they can be used to control the size and the aspect ratio of the obtained nanoparticles. Moreover, we have defined an optimal concentration of CTAB (50 mM) that allowed us to achieve AuNR with the most elongated shape. Our work will help researchers to prepare AuNR in a straightforward and more efficient way compared to what is commonly achieved, and at the same time makes use of a lower amount of CTAB. Despite the fact that in the present protocol CTAB is still needed and that must be removed from the surface for bio-related applications, our approach allows a substantial improvement in terms of costs, which could result in more scalable synthetic protocols and an easier diffusion of the new medical applications of AuNR.

Supporting Information

UV-Vis spectra of Au seeds. Viscosity of the growth solution in presence or without hydroquinone.

Histograms and the TEM images of the samples not shown in the text.

Acknowledgments Funding for this research was provided by Fondazione Cariplo (International Recruitment Call 2011, Project title: "An innovative, nanostructured biosensor for early diagnosis and minimal residual disease assessment of cancer, using Surface Enhanced Raman Spectroscopy") and by the Italian Ministry of Health under the frame of EuroNanoMed II (European Innovative Research & Technological Development Projects in Nanomedicine, project title: "InNaSERSS"). DP was partly supported by the Regional Foundation for Biomedical Research, Lombardia.

References

Alkilany AM, Nagaria PK, Hexel CR, Shaw TJ, Murphy CJ, Wyatt MD (2009) Cellular uptake and cytotoxicity of gold nanorods: molecular origin of cytotoxicity and surface effects. Small 5:701–708

Bao C, Beziere N, del Pino P, Pelaz B, Estrada G, Tian F, Ntziachristos V, de la Fuente JM, Cui D (2013) Gold nanoprisms as optoacoustic signal nanoamplifiers for in vivo bioimaging of gastrointestinal cancers. Small 9:68–74

Chen H, Shao L, Li Q, Wang J (2013) Gold nanorods and their plasmonic properties. Chem Soc Rev 42:2679–2724

Choi WI, Kim J-Y, Kang C, Byeon CC, Kim YH, Tae G (2011) Tumor regression in vivo by photothermal therapy based on gold-nanorod-loaded, functional nanocarriers. ACS Nano 5:1995–2003

Cobley CM, Chen J, Cho EC, Wang LV, Xia Y (2011) Gold nanostructures: a class of multifunctional materials for biomedical applications. Chem Soc Rev 40:44–56

Han G, Ghosh P, Rotello VM (2007) Functionalized gold nanoparticles for drug delivery. Nanomedicine 2:113–123

Howes PD, Rana S, Stevens MM (2014) Plasmonic nanomaterials for biodiagnostics. Chem Soc Rev 43:3835–3853

Huang HA, Barua S, Kay DB, Rege K (2009) Simultaneous enhancement of photothermal stability and gene delivery efficacy of gold nanorods using polyelectrolytes. ACS Nano 3:2941–2952

Katz E, Willner I (2004) Integrated nanoparticle-biomolecule hybrid systems: synthesis, properties, and applications. Angew Chem Int Ed 43:6042–6108

Kinnear C, Burnand D, Clift MJD, Kilbinger AFM, Rothen-Rutishauser B, Petri-Fink A (2014) Polyvinyl alcohol as a biocompatible alternative for the passivation of gold nanorods. Angew Chem Int Ed 53:12613–12617

Mehn D, Morasso C, Vanna R, Bedoni M, Prosperi D, Gramatica F (2013) Immobilised gold nanostars in a paper-based test system for surface-enhanced Raman spectroscopy. Vib Spectrosc 68:45–50

Morasso C, Mehn D, Vanna R, Bedoni M, Forvi E, Colombo M, Prosperi D, Gramatica F (2014) One-step synthesis of star-like gold nanoparticles for surface enhanced raman spectroscopy. Mater Chem Phys 143:1215–1221

Partanen A, Erola MOA, Mutanen J, Lajunen H, Suvanto S, Kuittinen M, Pakkanen TT (2015) Enhancing effects of gold nanorods on luminescence of dyes. J Lumin 157:126–130

Pelaz B, Grazu V, Ibarra A, Magen C, del Pino P, de la Fuente JM (2012) Tailoring the synthesis and heating ability of gold nanoprisms for bioapplications. Langmuir 28:8965–8970

Pérez-Hernández M, Del Pino P, Mitchell SG, Moros M, Stepien G, Pelaz B, Parak WJ, Gálvez EM, Pardo J, de la Fuente JM (2015) Dissecting the molecular mechanism of apoptosis during photothermal therapy using gold nanoprisms. ACS Nano 27:52–61

Perrault SD, Chan WCW (2009) Synthesis and surface modification of highly monodispersed, spherical gold nanoparticles of 50–200 nm. J Am Chem Soc 131:17042–17043

Polo E, del Pino P, Pelaz B, Grazua V, de la Fuente JM (2013) Plasmonic-driven thermal sensing: ultralow detection of cancer markers. Chem Commun 49:3676–3678

Ratto F, Matteini P, Rossi F, Pini R (2010) Size and shape control in the overgrowth of gold nanorods. J Nanopart Res 12:2029–2036

Rayavarapu RG, Ungureanu C, Krystek P, van Leeuwen TG, Manohar S (2010) Iodide impurities in hexadecyltrimethylammonium bromide (CTAB) products: lot–lot variations and influence on gold nanorod synthesis. Langmuir 26:5050–5055

Sau TK, Murphy CJ (2004) Seeded high yield synthesis of short Au nanorods in aqueous solution. Langmuir 20:6414–6420

Saute B, Premasiri R, Ziegler L, Narayanan R (2012) Gold nanorods as surface enhanced Raman spectroscopy substrates for sensitive and selective detection of ultra-low levels of dithiocarbamate pesticides. Analyst 137:5082–5087

Scarabelli L, Grzelczak M, Liz-Marzán LM (2013) Tuning gold nanorod synthesis through prereduction with salicylic acid. Chem Mater 25:4232–4238

Soliman MG, Pelaz B, Parak WJ, del Pino P (2015) Phase transfer and polymer coating methods toward improving the stability of metallic nanoparticles for biological applications. Chem Mater 27:990–997

Vigderman L, Zubarev ER (2013) High-yield synthesis of gold nanorods with longitudinal SPR peak greater than 1200 nm using hydroquinone as a reducing agent. Chem Mater 25:1450–1457

Walsh MJ, Barrow SJ, Tong W, Funston AM, Etheridge J (2015) Symmetry breaking and silver in gold nanorod growth. ACS Nano 9:715–724

Ye X, Jin L, Caglayan H, Chen J, Xing G, Zheng C, Doan-Nguyen V, Kang Y, Engheta N, Kagan CR, Murray CB (2012) Improved size-tunable synthesis of monodisperse gold nanorods through the use of aromatic additives. ACS Nano 6:2804–2817

Zou R, Zhang Q, Zhao Q, Peng F, Wang H, Yu H, Yang J (2010) Thermal stability of gold nanorods in an aqueous solution. Colloids Surf A 372:177–181